

Photo-Initiated Radical Hydrophosphination at Titanium Compounds Capable of Ti-P Insertion

Dennis M. Seth Jr. and Rory Waterman*

Department of Chemistry, University of Vermont, 82 University Pl, Burlington, VT 05405

ABSTRACT: Titanium compounds supported by the triamidoamine ligand (N_3N , $N(CH_2CH_2NSiMe_3)^3$) have been investigated for hydrophosphination catalysis. The simple titanium alkyl compound (N_3N)TiMe (**2**) demonstrate modest activity as a precatalyst for the photocatalytic hydrophosphination of styrene, but the terminal phosphido compound, (N_3N)TiPPh (**4**), is inactive. Analysis of these reactions by EPR spectroscopy indicates that (N_3N)TiMe undergoes homolytic Ti–C bond cleavage to achieve radical hydrophosphination. This pathway was further supported in a radical trapping experiment. The phosphido derivative **4** does not produce radicals under similar conditions, despite undergoing facile migratory insertion reactions with polar substrates featuring C–N and C–O multiple bonds. Both nitrile and isonitrile substrates insert with ultimate formation of phosphaalkene products, a change in reactivity as compared to the zirconium congener. Molecular structures of (N_3N)TiPPh (**4**), (N_3N)TiNBnC=PPh (**5**), and (N_3N)TiN(H)C(Ph)=PPh (**6**) are reported.

INTRODUCTION

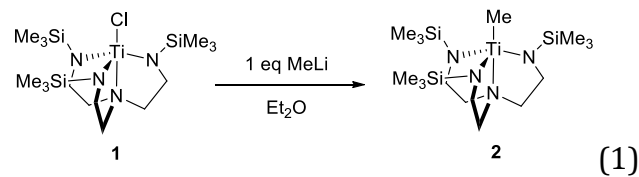
The efficient use of phosphorus is quickly becoming one of the most pressing issues of our time.¹ Among methods of producing phosphorus containing products, hydrophosphination stands strong as one of the most atom-economical and efficient reactions available, but unmet challenges loom for the transformation.² Despite a wide range of catalysts for the reaction,³ activity among catalysts has been modest in many cases with reactions requiring high reaction temperatures and extended times in many instances. Recently, a series of studies has demonstrated that irradiation of hydrophosphination is capable of not only accelerating this transformation but providing access to relatively inert substrates with zirconium- and copper-based catalysts.^{4, 5} Extending this methodology to other earth-abundant metals is thus a driving force in this field. Early work involving iron has been shown to be promising, with thermal hydrophosphination⁶ being greatly enhanced by photolysis.⁷ Thermal hydrophosphination using an iron β -diketiminate has also been shown to go through a radical-based mechanism.⁸

Initial exploration of titanium catalysts for hydrophosphination encourages greater use of this highly abundant transition metal. Mindiola reported a titanium phosphinidene compound that appears to operate through a [2+2] cycloaddition mechanism in the hydrophosphination of alkynes.⁹ LeGendre expanded on the substrate scope with titanium with the 1,4-hydrophosphination of 1,3-dienes with a Ti(II) catalyst.¹⁰ These examples also illustrate there is ample space for development of titanium-catalyzed hydrophosphination. In this report, we explore chemistry of triamidoamine-supported titanium compounds, based on those initially reported by Verkade^{11, 12} and Schrock,^{13, 14} respectively, due to their similarity to familiar zirconium congeners.¹⁵ Because photocatalytic hydrophosphination with zirconium compounds appears general,^{4, 16} catalysis under these conditions was of particular interest. While the Ti–P in this system is subject to migratory insertion, a new

phosphido derivative is not an active hydrophosphination catalyst. Unlike zirconium, the Ti–Me derivative promotes radical hydrophosphination under photolysis. This reactivity is more akin to radical hydrophosphination initiated by iron compounds as reported recently by Webster.⁸

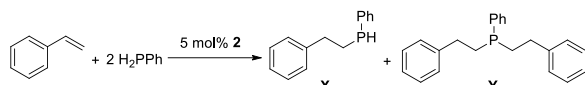
RESULTS AND DISCUSSION

Treatment of (N_3N)TiCl (**1**, $N_3N = N(CH_2CH_2NSiMe_3)^3$) with 1 equiv. of ethereal MeLi affords (N_3N)TiMe (**2**) in 91% yield as yellow crystals (eq. 1). The NMR spectra of **2** are simple, featuring an indicative methyl resonance at $\delta = 1.00$ and methylene triplets at $\delta = 3.35, 2.16$ in the 1H NMR spectrum. Spectra of **2** are consistent with related derivatives.^{11, 13, 14, 17}



Initial hydrophosphination reactions were undertaken with styrene and phenylphosphine as substrates using 5 mol % **2** (Table 1). While catalysis was observed under ambient conditions (light and temperature), conversions were substantially higher under irradiation in both the visible and near ultraviolet. The reaction exclusively affords the anti-Markovnikov product. Decreasing the excess of phosphine lead to a mild decrease in selectivity, but the reaction remains selective to the single activation product. Control reactions demonstrated that light, and in particular photon density, is a critical factor in the observed reactivity.

Table 1 Reaction Condition Screening for Hydrophosphination of Styrene with Phenylphosphine



conditions ^a	t	X	Y
Dark	5 h	< 1 %	0 %
Dark, 75°C	5 h	16 %	0 %
Ambient	5 h	36 %	5 %
360 nm UV	1 h	22 %	trace
Blue LED can	1 h	63 %	2 %
LED Lamp	1 h	40 %	4 %

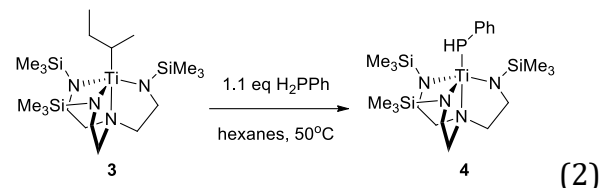
^aAll reactions were run in benzene-*d*₆ solvent and temperature was monitored such that no runs were greater than 35 °C unless noted. Conversions were determined by integrating the ¹H and ³¹P{¹H} NMR spectra. Control reactions without catalyst give trace yields, consistent with prior studies.¹⁸

It was initially hypothesized that catalysis would occur via substrate insertion into a Ti–P bond. Observation of this catalysis by ³¹P NMR spectroscopy did not reveal an apparent titanium-phosphido intermediate, despite the relatively high loading. The absence of a clear phosphido compound is consistent with a developing hypothesis that many hydrophosphination precatalysts would have greater reactivity if not for sluggish activation, i.e. conversion of the precatalyst to an active metal-phosphido derivative.¹⁵ To test both of these hypotheses, the preparation of a phosphido derivative was undertaken.

Treatment of **2** with either 1 equiv. or excess phenylphosphine failed to form a titanium phosphido product, and the only new resonances observed in ³¹P NMR spectra of these attempts were small amounts of dehydrocoupling products. For (N₃N)Zr derivatives, the alkyl compounds do not directly react with P–H bonds because cyclometalation of the triamidoamine ligand occurs faster to afford [κ⁵-N,N,N,N,C-(Me₃SiNCH₂CH₂)₂NCH₂CH₂NSiMe₂CH₂]Zr rather than direct reaction with phosphine.¹⁹ Thus, (N₃N)Ti(^tBu) (**3**), a precursor known to cyclometallate,¹³ was used instead. Treatment of **3** with 1.1 equiv. of phenylphosphine in hexanes solution resulted in a color change to a deep red upon heating to 50 °C. Analytically pure, deep red crystals of (N₃N)TiPPh (**4**) were obtained in 88% yield upon crystallization from pentane solution at –40 °C (eq. 2). Spectroscopic data confirms the formulation, featuring diagnostic resonances at δ = 9.1 and δ = 4.59 in the ³¹P{¹H} and ¹H NMR spectra, respectively, associated with the phenylphosphido ligand, and ν_{PH} = 2293 cm^{–1} was measured in the infrared. An expected LMCT band was observed at λ = 508 nm (ε = 2,300 M^{–1}cm^{–1}) with an intense feature in the near UV λ = 322 nm (ε = 11,000 M^{–1}cm^{–1}).

Crystals suitable for X-ray analysis were obtained by slow crystallization from cold pentane solution of **4**, and molecular structure is shown in Figure 1. The key bond of **4**, Ti1–P1 = 2.563(1) Å, is significantly longer than that of the cationic titanocene phosphido reported by LeGendre (Ti–P = 2.3599(14) Å).²⁰ This increased bond length is consistent with the upfield shift of the ³¹P NMR resonance of **4** and with the limited ligand-to-metal π-bonding found for (N₃N)ZrPRR' compounds, though charge may play a role in these bond lengths as well.¹⁹ Geometry index²¹ calculations allow for the determination of the geometry at a 5 coordinate metal center on a range from square pyramidal ($\tau_5 = 0$) to trigonal bipyramidal ($\tau_5 = 1$). This

calculation shows $\tau_5(\text{Ti}) = 0.955$ versus $\tau_5(\text{Zr}) = 1.02$,²² which indicate that both complexes show a distorted trigonal bipyramidal geometry.¹⁹



With a titanium phosphido in hand, catalysis testing was performed to determine the role of **4** for catalytic hydrophosphination under irradiation. A reaction of phenylphosphine with styrene with 5 mole % of **4** was prepared and divided into four equal parts, with deliberate irradiation in each the visible (LED lamp) and near-UV centered at 360 nm, under ambient light, and a control in the dark. In the dark, no appreciable reactivity was observed over extended reaction times (24 h). Ambient lighting saw no conversion under similar reaction times to those for **2**. After 1 h, both LED and 360 nm light showed no appreciable conversion to a hydrophosphination product, though **4** did disappear to produce an as-yet unidentified resonance at δ ~ –121.3 in ³¹P{¹H} NMR.

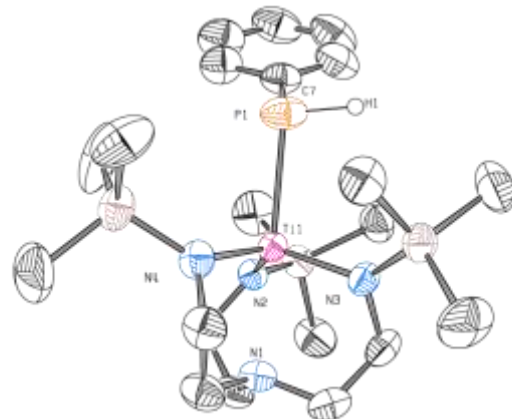
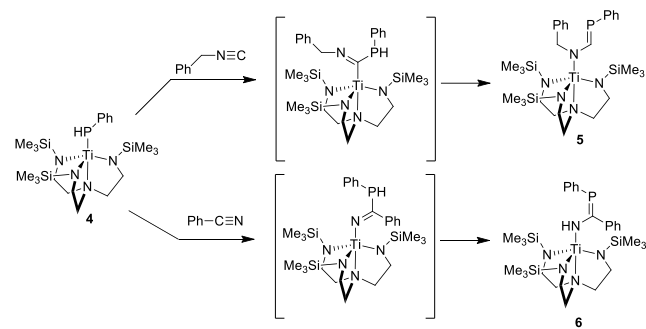


Figure 1. ORTEP diagram of the molecular structure of **4** with thermal ellipsoids generated at the 50% probability level. All hydrogen atoms except H1 omitted for clarity.

To explore if the Ti–P bond is viable for insertion, model stoichiometric reactions were performed. Treatment of **4** with benzyl isocyanide at ambient temperature in toluene solution resulted in an immediate color change from deep red to deep orange-brown. Large, block shaped crystals of **5** formed from a layered solution of pentane over toluene in modest yield (45%), likely due to the lipophilicity of the product and an unoptimized crystallization technique (Scheme 1). The molecular structure of **5** is shown in Figure 2. The geometry of the structure indicates that the isocyanide reacted with the titanium phosphido via a 1,1-insertion followed by a subsequent rearrangement. The phosphphaalkene bond, P1–C1 = 1.717(22) Å is consistent with, if not slightly longer than, published phosphphaalkenes,²³ and similar to the isostructural zirconium compounds.²⁴ The short C1–N1 bond length of 1.385 Å as well as the near-planarity of the Ti1–N1–C1–P1 system, as shown by dihedral angle of –168.54°, indicates significant conjugation. The phosphphaalkene moiety is confirmed spectroscopically with diagnostic

resonances at $\delta = 10.55$, $\delta = 198.6$, and $\delta = 92.5$ for ^1H , $^{13}\text{C}\{^1\text{H}\}$, and $^{31}\text{P}\{^1\text{H}\}$ NMR spectra, respectively. Unfortunately, the predicted P=C stretch ($\sim 900 \text{ cm}^{-1}$) appears to be obscured by the triamidoamine backbone in the infrared.



Scheme 1 Stoichiometric insertion reactions of at the Ti–P bond of **4**.

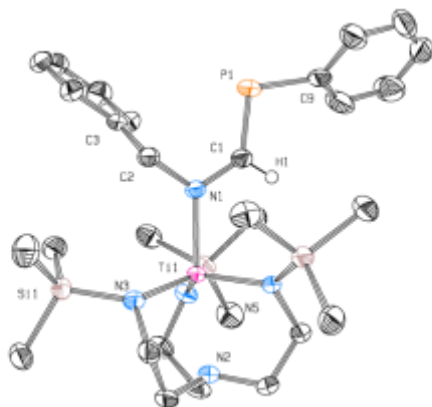


Figure 2. ORTEP structure of **5**. All hydrogens except H1, which was located from the electron difference map, omitted for clarity. Thermal ellipsoids generated at the 50% probability level.

Alternatively, the reaction of **4** with benzonitrile in benzene-*d*₆ occurred slowly over approximately 18 h. The product of the insertion, $(\text{N}_3\text{N})\text{TiN}(\text{H})\text{C}(\text{Ph})=\text{PPH}$ (**6**) is shown in Figure 3. In this instance, a 1,2-insertion product forms, but somewhat surprisingly, the phosphaalkene tautomer is favored as the product. This was identified by the imine $\nu_{\text{NH}} = 3247 \text{ cm}^{-1}$ in the infrared. Diagnostic resonances in the NMR spectra are also seen including the imine hydrogen at $\delta = 9.02$ and the phosphorus resonance $\delta = 86.74$. The spectroscopic assignment was confirmed through X-ray crystallographic analysis. Like compound **5**, a P1–C1–N1–Ti1 dihedral angle = $-169.02(8)$ and $\text{P1–C1} = 1.735(1) \text{ \AA}$ indicate the phosphaalkene moiety and extended conjugation. This reactivity is in stark contrast with the zirconium analog, which prefers the other tautomer,²⁵ but is more consistent with analogous thorium reactivity.²⁶

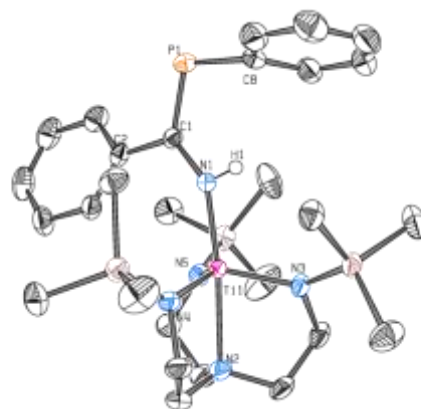
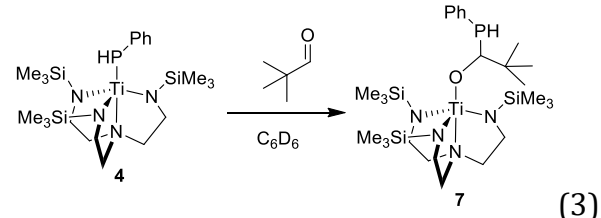
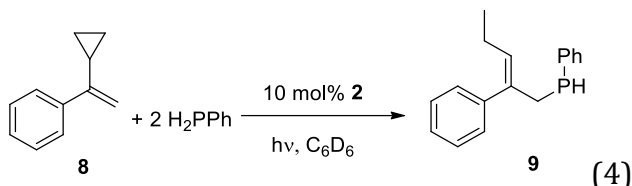


Figure 3. ORTEP structure of **6**. All hydrogens except H1 omitted for clarity. Thermal ellipsoids generated at 50% probability

Finally, a simple reaction between phosphido **4** and pivalaldehyde was conducted in benzene-*d*₆. The solution immediately became light yellow upon addition of the pivalaldehyde, and yellow crystals were collected by crystallization from concentrated pentane solution (eq. 3). The insertion product was assigned, in part, by $\nu_{\text{PH}} = 2310 \text{ cm}^{-1}$ observed in the infrared, a indicative secondary ^{31}P NMR resonance at $\delta = -51.8$ (*cf.* PhMePH has $\delta = -68.4$),²⁷ and a corresponding phosphine resonance in the ^1H NMR spectrum at $\delta = 4.76$ with diagnostic couplings ($|\text{J}_{\text{PH}}| = 203.6, 4.5 \text{ Hz}$). Unfortunately, single crystals of **7** were not able to provide satisfactory diffraction data for a molecular structure to confirm the spectroscopic data.



In light of observed insertion into the Ti–P bond, it became apparent that methyl compound **2** was undergoing unique reactivity that needed to be addressed. The first hypothesis was the potential for radical chemistry due to the facile Ti(III/IV) couple for many organometallic compounds. Webster has recently demonstrated effective use of the cyclopropyl substituent as a radical trap to corroborate radical-based hydrophosphination.⁸ Thus, α -cyclopropyl styrene (**8**) was synthesized²⁸ and tested for hydrophosphination with phenylphosphine. Reaction of **8** with 2 equiv. of phenylphosphine and 10 mol % of **2** in benzene-*d*₆. After 1 h, the starting material was consumed (eq. 3), as shown by the loss of the characteristic resonances in the ^1H NMR spectrum (Figure S29). Instead, an allyl phosphine has been synthesized as tentatively assigned by a triplet at $\delta = 5.56$ with a phosphine resonance at $\delta = 4.10$ ^1H NMR spectrum, and a characteristic secondary phosphine resonance at $\delta = -55.26$ in $^{31}\text{P}\{^1\text{H}\}$ spectrum (Figure S30). The spectral data points to cyclopropane ring opening during the reaction, consistent with a radical-based mechanism.



A final experiment established that open-shell compounds are indeed being generated during catalysis. Reaction of **8** with phenylphosphine in the presence of 10 mol % of **2** in pentane solution was conducted in an EPR tube. At the onset of the reaction, there were no signals in an ambient temperature EPR spectrum. When the reaction mixture was illuminated with a broadband UV lamp in the EPR spectrometer; however, features appear immediately, indicating that radicals are generated under reaction conditions (Figure S27). Control reactions determine that **2** is capable of homolytic cleavage under light, which is consistent with prior reports.²⁹ Additionally, no signal is observed during irradiation of a mixture of **8** and phenylphosphine. It is therefore proposed that Ti–C cleavage event occurs that leads to radical hydrophosphination.

CONCLUSION

Titanium compounds were known to engage in catalytic hydrophosphination, and the activity with styrene represents the most challenging substrate for this category of catalyst to date. However, the triamidoamine-supported titanium methyl precatalyst **2** appears to undergo Ti–C bond cleavage upon irradiation that generates radical intermediates that initiate hydrophosphination. Because similar metal-initiated radical hydrophosphination reactivity has already been reported for iron compounds by Webster, such reactivity may be a general pitfall for these most abundant 3d metals, though opportunity can be envisioned at this point as well. Nevertheless, clean 1,1- and 1,2-insertion reactivity of the Ti–P bond of **4** is encouraging for developing more active titanium-based hydrophosphination catalysts. The direct formation of a phosphaalkene from a nitrile was unexpected but not unprecedented based on Walensky’s thorium work. The difference from zirconium is, however, encouraging for identifying uniquely titanium-based reactivity.

EXPERIMENTAL SECTION

All reactions were performed under a dry nitrogen atmosphere using an MBraun glovebox or standard Schlenk techniques unless otherwise noted. All solvents were degassed with nitrogen, run through an alumina column, and stored over activated 3 Å molecular sieves. Phenylphosphine (CAS: 638-21-1) and all substrates were used as received. The compounds (N₃N)H₃,³⁰ (N₃N)TiCl,¹⁴ (N₃N)TiBu¹⁴ were prepared in a satisfactory manner from literature methods. Celite-454® was purchased and heated to 180 °C under dynamic vacuum overnight before use. NMR spectra were collected on a Bruker AXR 500 MHz spectrometer in benzene-*d*₆ solution unless otherwise noted and are reported with reference to residual solvent signals (benzene-*d*₆, δ 7.16 and 128.0) or to an external standard of 85% H₃PO₄ (δ 0.0) for ³¹P NMR spectra. Infrared spectra were collected on a Bruker Alpha FT-IR spectrometer with an ATR head. Absorption spectra were recorded with an Agilent Technologies Cary 100 Bio UV-Visible Spectrophotometer (Santa Clara, CA, USA). Elemental analysis data was collected on a Vario MicroCube with acetonilide as a standard. EPR data were collected on a Bruker EMXplus EPR spectrometer equipped with an optical cavity. X-ray diffraction data were collected on a Bruker APEX 2 CCD platform diffractometer [Mo Kα (λ = 0.71073 Å)]. Experimental details regarding light sources in this study have been described previously.¹⁸

Synthesis of (N₃N)TiMe (2). A 4-dram scintillation vial was charged with 0.552 g of (N₃N)TiCl (1.24 mmol) and ~10 mL of pentane. The resulting deep orange solution was cooled to -40 °C, whereupon 1 mL of 1.24 M methyl lithium in diethyl ether solution (1.24 mmol) was added. The reaction was shaken and became a cloudy orange. After resting for ca. 16 hours at room temperature, the solution was pulled through a short (~1 cm) plug of alumina and concentrated to yield 0.524 g (quant.) of yellow-orange residue as crude product. The residue was extracted into minimal pentane, the solution filtered and cooled to -40 °C for at least 12 h to afford 0.477 g (91%) of yellow, block-like crystals that were isolated from the mother liquor. Repeated efforts for satisfactory analysis failed, despite apparently pure compound by NMR spectroscopy. ¹H NMR (500 MHz, C₆D₆) δ 3.35 (t, 6 H, CH₂), 2.16 (t, 6 H, CH₂), 1.00 (s, 3 H, TiCH₃), 0.31 (s, 27 H, SiCH₃). ¹³C NMR (126 MHz, C₆D₆) δ 61.34 (s, CH₂), 49.96 (s, CH₂), 48.15 (s, TiCH₃), 1.10 (s, SiCH₃). IR (KBr): 2944.90 (w), 2845.89 (w), 1242.53 (m), 1052.83 (m), 926.27 (m), 900.37 (s), 823.06 (s), 781.18 (s), 743.05 (s). Anal. Calcd for C₁₆H₄₂N₄Si₃Ti: C, 45.47; H, 10.02; N, 13.26. Found: C, 44.11; H, 9.799; N, 13.22.

Synthesis of (N₃N)TiPPh₃ (4). A Teflon valved 250 mL reaction flask was charged with 700 mg of (N₃N)TiⁱBu (1.49 mmol) dissolved in 15 mL of hexanes. To this was added 172 μL of phenylphosphine (1.56 mmol, 1.05 eq). The reaction was taken out of the glovebox and placed into an oil bath at 50 °C for 4 h. During this time, the solution changed color from orange to an extremely deep, opaque red-orange. The solution was brought into the glovebox, filtered through Celite, and the solution concentrated to incipient crystallization. The solids were redissolved, and the solution cooled to -40 °C for ca. 16 h, whereupon 670 mg (1.31 mmol, 87.6%) of dark red-orange needle-like crystals had formed. X-ray quality crystals were grown from slow evaporation of a pentane solution of **4**. ¹H NMR (500 MHz, C₆D₆) δ 7.65 (t, |J| = 7.5 Hz, 2 H, *m*-C₆H₅), 7.12 (dd, |J| = 10.9, 4.4 Hz, 2 H, *o*-C₆H₅), 6.94 (t, *J* = 7.4 Hz, 1 H, *p*-C₆H₅), 4.59 (d, |J| = 207.6 Hz, 1 H, PH), 3.42 (m, 6 H, CH₂), 2.17 (m, 6 H, CH₂), 0.33 (s, 27 H, SiCH₃). ¹³C{¹H} NMR (126 MHz, C₆D₆): δ 132.27 (aryl), 132.17 (aryl), 123.70 (aryl), 63.41, 50.37 (CH₂), 50.35 (CH₂), 1.41 (CH₃). Some aryl carbons are obscured by residual solvent signal. ³¹P{¹H} NMR (202 MHz, C₆D₆) δ 8.35 (s). IR (KBr): 3057.31 (w), 2949.80 (m), 2891.24 (m), 2851.92 (m), 2292.53 (w), 1580.26 (w), 1058.26 (w), 1240.17 (s), 1045.75 (s), 997.00 (s), 825.14 (s), 777.77 (s), 731.23 (s). Anal. Calcd for C₂₁H₄₅N₄PSi₃Ti: C, 48.81; H, 8.78; N, 10.84. Found: C, 47.91; H, 9.424; N, 11.92.

Synthesis of (N₃N)TiN(Bn)C(H)=PPh (5). A 1 dram scintillation vial was charged with 92.1 mg of (N₃N)TiPPh₃ (0.178 mmol), dissolved in ca. 0.5 mL toluene. Benzyl isocyanide (20.8 mg, 0.178 mmol) was added neat, and the solution changed color from a deep-red to a deep-orange. The reaction was layered with ca 1mL pentane and carefully placed into a -40 °C freezer for ca. 16 hours. During this time, 50.3 mg (0.0794 mmol, 44.6%) of well-defined, deep orange-red crystals formed. A suitable crystal was taken for X ray analysis from this crystallization. ¹H NMR (500 MHz, C₆D₆) δ 10.55 (d, *J* = 13.7 Hz, 1 H, P=CH), 7.85 (t, *J* = 6.6 Hz, 2 H, Aryl), 7.59 (d, *J* = 7.6 Hz, 2 H, aryl), 7.30 (t, *J* = 7.7 Hz, 2 H, aryl), 7.15–7.08 (m, 2 H, aryl, obscured by residual solvent signal), 5.47 (s, 2 H, PhCH₂), 3.42 (m, 6 H, CH₂), 2.36 (m, 6 H, CH₂), 0.19 (s, 27 H, SiCH₃). ¹³C NMR (126 MHz, C₆D₆): δ 198.57(P=C), 145.40 (aryl), 138.40 (aryl), 132.45 (aryl), 127.7 (aryl), 126.02 (aryl), 64.00 (CH₂), 59.02 (PhCH₂), 49.35 (CH₂), 1.19 (CH₃). ³¹P{¹H} NMR (202 MHz, C₆D₆) δ 92.52 (s). IR (KBr): 3054.66 (w), 2947.58 (m), 2887.46 (m), 2863.10 (m), 2846.35 (m), 1581.10 (w), 1368.21 (m), 826.82 (s), 780.37 (s), 734.87 (s). Anal. Calcd for C₂₉H₅₂N₅PSi₃Ti: C, 54.95; H, 8.27; N, 11.05. Found: C, 54.97; H, 8.492; N, 11.97.

Synthesis of (N₃N)TiN(H)C(Ph)=PPh (6). To a Teflon-sealed NMR tube was added 64.2 mg of (N₃N)TiPPh₃ (0.124 mmol), 13 μL of benzonitrile (0.124 mmol, 1 equiv.), and ca. 1 mL of benzene-*d*₆. There was no immediate color change. The reaction was monitored by ³¹P{¹H} and ¹H NMR spectroscopy, and after 18 h, all the starting material had been consumed. The reaction was brought into the glovebox and lyophilized. The residue was taken up with minimal pentane and allowed to crystalize in the freezer. The yield was 58.2 mg (75.8%) of deep red crystals. X-ray quality crystals were grown from a saturated toluene solution with pentane layered upon it. ¹H NMR (500 MHz,

C_6D_6) δ 9.02 (s, 1 H, *NH*), 8.28 (dd, $|J|$ = 7.2, 1.8 Hz, 2 H, aryl), 7.88 (dd, $|J|$ = 6.6, 4.8 Hz, 2 H, aryl), 7.27 (t, $|J|$ = 7.5 Hz, 2 H, aryl), 7.21–7.08 (m, obscured by residual solvent signal), 3.18 (t, $|J|$ = 5.3 Hz, 6 H, CH_2), 2.35 (t, $|J|$ = 5.3 Hz, 6 H, CH_2), 0.06 (s, 27 H, $SiCH_3$). ^{13}C NMR (126 MHz, C_6D_6): δ = 143.36 (aryl), 142.09 (aryl), 135.76 (aryl), 129.16 (aryl), 128.74 (aryl), 129.16 (aryl), 127.76 (aryl), 127.14 (aryl), 62.21 (CH_2), 49.62 (CH_2), 0.85 ($SiCH_3$). Some carbons are obscured by residual solvent signal. $^{31}P\{^1H\}$ NMR (202 MHz, C_6D_6) δ 86.74 (s). IR (KBr): 3247.82 (w), 3066.14 (w), 3051.34 (w), 3010.45 (w), 2943.40 (w), 2893.44 (w), 2860.01 (w), 1587.99 (m), 1479.44 (m), 1446.21 (m), 790.15 (s), 744.37 (s), 691.82 (s). Anal. Calcd for $C_{28}H_{50}N_3PSi_3Ti$: C, 54.26; H, 8.13; N, 11.30. Found: C, 53.93; H, 8.964; N, 11.52.

Synthesis of $(N_3N)TiOCH(tBu)PPh_3$ (7). To a Teflon-capped NMR tube was added 83.5 mg $(N_3N)TiPPh_3$ (0.162 mmol), ca. 1 mL benzene- d_6 , and 18 μ L of pivalaldehyde (0.1656 mmol, 1.02 eq), to be monitored by NMR over time. The solution immediately lightened to a clear brown, and NMR indicated complete conversion. The tube was transferred back into the glovebox, and the solution was lyophilized, dissolved into pentane and stuck in the freezer to yield 74.5 mg (74.7%) of yellow crystals. 1H NMR (500 MHz, C_6D_6) δ 7.66 (dd, $|J|$ = 10.1, 4.0 Hz, 2 H, aryl), 7.15–7.11 (m, 2H, aryl), 7.05 (t, $|J|$ = 7.4 Hz, 1 H, aryl), 5.45 (dd, $|J|$ = 4.4, 2.9 Hz, 1 H, CH), 4.76 (dd, $|J|$ = 203.6, 4.5 Hz, 1H, PH), 3.18 (qdd, $|J|$ = 13.5, 6.2, 4.8 Hz, 6 H, CH_2), 2.50 (m, 6 H, CH_2), 1.22 (s, 9 H, CH_3), 0.38 (s, 27 H, $SiCH_3$). ^{13}C NMR (126 MHz, C_6D_6): δ 137.06 (aryl), 134.58 (aryl), 127.94 (aryl), 97.79 (OC), 62.88 (CH_2), 49.44 (CH_2), 39.40 (CCH_3), 28.28 (CCH_3), 1.75 ($SiCH_3$). ^{31}P NMR (202 MHz, C_6D_6) δ –51.85 (s). IR (KBr): 3068.92 (w), 3052.17 (w), 2949.30 (m), 2889.47 (m), 2849.38 (m), 2310.22 (m), 1294.49 (s), 870.55 (s), 825.89 (s), 781.03 (s), 734.07 (s), 712.06 (m). Anal. Calcd for $C_{26}H_{55}N_4OPSi_3Ti$: C, 51.80; H, 9.20; N, 9.29. Found: C, 51.05; H, 9.203; N, 9.56.

Synthesis of α -cyclopropyl styrene (8)³¹ Prepared by a modification of literature procedure.²⁸ To a 50 mL round bottom flask in the glovebox was added 4.110 g of methyl triphenylphosphonium bromide (11.51 mmol), 1.286 g of potassium *tert*-butoxide (11.48 mmol), and ca. 30 mL of tetrahydrofuran. The yellow reaction mixture was capped and stirred for 30 min, after which 1.33 g of cyclopropyl phenyl ketone (9.11 mmol, 0.8 equiv.) was added slowly. After stirring for ~16 h, the reaction was removed from the glovebox and quenched by pouring into a separatory funnel with 50 mL distilled water. The reaction was extracted 4 x 25 mL diethyl ether. Organic extracts were combined and dried over sodium sulfate, and concentrated to yield a crude oil and solids. The crude product was purified by flash chromatography (silica, 9:1 hex:EtOAc, R_f = 0.81) to yield 1.19 g (91%) of light yellow liquid. Spectra of the product matched literature values.²⁸

Synthesis of phenyl(2-phenylpent-2-en-1-yl)phosphine (9) In the glovebox, to a 2 dram shell vial was added 213 μ L phenylphosphine (1.94 mmol), 139 mg **8** (0.969 mmol), 40.8 mg **2** (10 mol %), and ca. 0.5 mL benzene- d_6 . The reaction was transferred into an NMR tube and was monitored by 1H and $^{31}P\{^1H\}$ NMR. The reaction was placed into a blue LED photoreactor, and after 1 hour all of the reactant alkene was consumed by 1H NMR. Attempted purification by adding methanol and 30% hydrogen peroxide yielded violent foaming and decomposition. Partial characterization is as follows: 1H NMR (500 MHz, C_6D_6) δ 5.56 (t, J = 6.2 Hz, 1H), 4.11 (dt, J = 207.7, 7.4 Hz, P-H), 2.88 (m, 2H), 1.84 (m, 3H), 0.80 (t, J = 7.5 Hz, 3H). $^{31}P\{^1H\}$ NMR (202 MHz, C_6D_6) δ –55.26 (s). HRMS calcd for $C_{17}H_{19}P$: 255.1292 [MH]⁺, found 255.1296.

General Protocol for Catalytic Runs

To a two-dram shell vial was added 35 μ L of styrene, 0.5 mL benzene- d_6 spiked with 1,3,5-trimethoxybenzene, 67 μ L phenylphosphine, and 6 mg **2**. The mixture was transferred to an NMR tube and subject to reaction conditions, irradiation, dark, or ambient lighting, and monitored by 1H and $^{31}P\{^1H\}$ NMR spectroscopy. Completion was measured by the disappearance of styrene resonances, and conversion to hydrophosphination products were determined by integrating the phosphine signals. Thermal trials were done in a J-Young style NMR tube.

General Protocol for EPR Experiment

Prepared according to general procedure with the exception that the reaction mixture was in an EPR tube, the solvent was pentane, and the

reaction mixture was irradiated with a Bruker ER 203V lamp accessory and monitored by EPR spectroscopy.

ASSOCIATED CONTENT

Supporting Information

Representative spectra of compounds and crystallographic data table (PDF). Full crystallographic data for compounds **4**, **5**, and **6** as CCDC 2237685–2237687, respectively (CIF). The Supporting Information is available free of charge on the ACS Publications website.

AUTHOR INFORMATION

Corresponding Author

*rory.waterman@uvm.edu

The authors declare no competing financial interest

ACKNOWLEDGMENT

This research was supported by the U. S. National Science Foundation through CHE-2101766, and by the Japan Society for the Promotion of Science. EPR measurements were conducted in a spectrometer with optical cavity that was obtained through CHE-1919417.

REFERENCES

- Cordell, D.; White, S. Peak Phosphorus: Clarifying the Key Issues of a Vigorous Debate about Long-Term Phosphorus Security. *Sustainability* **2011**, 3 (10), 2027.
- (a) Bange, C. A.; Waterman, R. Challenges in Catalytic Hydrophosphination. *Chemistry* **2016**, 22 (36), 12598–12605, <https://doi.org/10.1002/chem.201602749>. (b) Lau, S.; Hood, T. M.; Webster, R. L. Broken Promises? On the Continued Challenges Faced in Catalytic Hydrophosphination. *ACS Catal* **2022**, 12 (17), 10939–10949.
- Novas, B. T.; Waterman, R. Metal-Catalyzed Hydrophosphination. *ChemCatChem* **2022**, 14 (22), e202200988, <https://doi.org/10.1002/cctc.202200988>.
- (a) Bange, C. A.; Conger, M. A.; Novas, B. T.; Young, E. R.; Liptak, M. D.; Waterman, R. Light-Driven, Zirconium-Catalyzed Hydrophosphination with Primary Phosphines. *ACS Catalysis* **2018**, 8 (7), 6230–6238. (b) Novas, B. T.; Morris, J. A.; Liptak, M. D.; Waterman, R. Effect of Photolysis on Zirconium Amino Phenoxides for the Hydrophosphination of Alkenes: Improving Catalysis. *Photochem* **2022**, 2 (1), 77–87. (c) Novas, B. T.; Bange, C. A.; Waterman, R. Photocatalytic Hydrophosphination of Alkenes and Alkynes Using Diphenylphosphine and Triamidoamine-Supported Zirconium. *European Journal of Inorganic Chemistry* **2018**, 2019 (11–12), 1640–1643, <https://doi.org/10.1002/ejic.201801079>.
- Dannenberg, S. G.; Waterman, R. A bench-stable copper photocatalyst for the rapid hydrophosphination of activated and unactivated alkenes. *Chem Commun (Camb)* **2020**, 56 (91), 14219–14222, 10.1039/D0CC06570F.
- Kamitani, M.; Itazaki, M.; Tamiya, C.; Nakazawa, H. Regioselective double hydrophosphination of terminal arylacetylenes catalyzed by an iron complex. *J Am Chem Soc* **2012**, 134 (29), 11932–11935.
- (a) Ackley, B. J.; Pagano, J. K.; Waterman, R. Visible-light and thermal driven double hydrophosphination of terminal alkynes using a commercially available iron compound. *Chem Commun (Camb)* **2018**, 54 (22), 2774–2776, 10.1039/C8CC00847G. (b) Pagano, J. K.; Bange, C. A.; Farmiloe, S. E.; Waterman, R. Visible Light Photocatalysis Using a Commercially Available Iron Compound. *Organometallics* **2017**, 36 (20), 3891–3895.
- Espinal-Viguri, M.; King, A. K.; Lowe, J. P.; Mahon, M. F.; Webster, R. L. Hydrophosphination of Unactivated Alkenes and

Alkynes Using Iron(II): Catalysis and Mechanistic Insight. *ACS Catalysis* **2016**, *6* (11), 7892-7897.

(9) Zhao, G.; Basuli, F.; Kilgore, U. J.; Fan, H.; Aneetha, H.; Huffman, J. C.; Wu, G.; Mindiola, D. J. Neutral and zwitterionic low-coordinate titanium complexes bearing the terminal phosphinidene functionality. Structural, spectroscopic, theoretical, and catalytic studies addressing the Ti-P multiple bond. *J Am Chem Soc* **2006**, *128* (41), 13575-13585.

(10) Perrier, A.; Comte, V.; Moise, C.; Le Gendre, P. First titanium-catalyzed 1,4-hydrophosphination of 1,3-dienes. *Chemistry* **2010**, *16* (1), 64-67, <https://doi.org/10.1002/chem.200901863>.

(11) Duan, Z.; Naiimi, A. A.; Lee, J.-H.; Verkade, J. G. Novel Volatile Azatranes of Group 4 Metals. *Inorganic Chemistry* **2002**, *34* (22), 5477-5482.

(12) Duan, Z.; Verkade, J. G. Synthesis and Characterization of a Novel Azatitanatane. *Inorganic Chemistry* **2002**, *34* (17), 4311-4316.

(13) Cummins, C. C.; Schrock, R. R.; Davis, W. M. Synthesis of vanadium and titanium complexes of the type $RM[(Me_3SiNCH_2CH_2)_3N]$ ($R = Cl$, alkyl) and the structure of $CIV[(Me_3SiNCH_2CH_2)_3N]$. *Organometallics* **2002**, *11* (4), 1452-1454.

(14) Schrock, R. R.; Cummins, C. C.; Wilhelm, T.; Lin, S.; Reid, S. M.; Kol, M.; Davis, W. M. Synthesis of Titanium Complexes That Contain Triamido-Amine Ligands. *Organometallics* **1996**, *15* (5), 1470-1476.

(15) Waterman, R. Triamidoamine-Supported Zirconium Compounds in Main Group Bond-Formation Catalysis. *Acc Chem Res* **2019**, *52* (8), 2361-2369.

(16) Bange, C. A.; Waterman, R. Zirconium-Catalyzed Intermolecular Double Hydrophosphination of Alkynes with a Primary Phosphine. *ACS Catalysis* **2016**, *6* (10), 6413-6416.

(17) Waterman, R. Selective Dehydrocoupling of Phosphines by Triamidoamine Zirconium Catalysts. *Organometallics* **2007**, *26* (10), 2492-2494. Paparo, A.; van Kruchten, F. D.; Spaniol, T. P.; Okuda, J. Formate complexes of titanium(iv) supported by a triamido-amine ligand. *Dalton Trans* **2018**, *47* (10), 3530-3537.

(18) Dannenberg, S. G.; Seth, D. M., Jr.; Finfer, E. J.; Waterman, R. Divergent Mechanistic Pathways for Copper(I) Hydrophosphination Catalysis: Understanding That Allows for Diastereoselective Hydrophosphination of a Tri-substituted Styrene. *ACS Catalysis* **2023**, *13* (1), 550-562.

(19) Roering, A. J.; Maddox, A. F.; Elrod, L. T.; Chan, S. M.; Ghebreab, M. B.; Donovan, K. L.; Davidson, J. J.; Hughes, R. P.; Shalumova, T.; MacMillan, S. N.; et al. General Preparation of $(N_3N)ZrX$ ($N_3N = N(CH_2CH_2NSiMe_3)_3$) Complexes from a Hydride Surrogate. *Organometallics* **2008**, *28* (2), 573-581.

(20) Normand, A. T.; Bonnin, Q.; Brandes, S.; Richard, P.; Fleurat-Lessard, P.; Devillers, C. H.; Balan, C.; Le Gendre, P.; Kehr, G.; Erker, G. The Taming of Redox-Labile Phosphidotitanocene Cations.

Chemistry **2019**, *25* (11), 2803-2815, <https://doi.org/10.1002/chem.201805430>.

(21) Addison, A. W.; Rao, T. N.; Reedijk, J.; van Rijn, J.; Verschoor, G. C. Synthesis, structure, and spectroscopic properties of copper(II) compounds containing nitrogen-sulphur donor ligands; the crystal and molecular structure of aqua[1,7-bis(N-methylbenzimidazol-2'-yl)-2,6-dithiaheptane]copper(II) perchlorate. *J. Chem. Soc., Dalton Trans.* **1984**, (7), 1349-1356, 10.1039/DT9840001349.

(22) Roering, A. J.; MacMillan, S. N.; Tanski, J. M.; Waterman, R. Zirconium-catalyzed heterodehydrocoupling of primary phosphines with silanes and germanes. *Inorg Chem* **2007**, *46* (17), 6855-6857.

(23) Han, Z.; Rohner, D.; Samedov, K.; Gates, D. P. Isolable Phosphaalkenes Bearing 2,4,6-Trimethoxyphenyl and 2,6-Bis(trifluoromethyl)phenyl as P-Substituents. *J Org Chem* **2020**, *85* (22), 14643-14652.

(24) (a) MacMillan, S. N.; Tanski, J. M.; Waterman, R. Insertion of benzyl isocyanide into a Zr-P bond and rearrangement. Atom-economical synthesis of a phosphaalkene. *Chem Commun (Camb)* **2007**, (40), 4172-4174, 10.1039/B709506F. (b) Roering, A. J.; Elrod, L. T.; Pagano, J. K.; Guillot, S. L.; Chan, S. M.; Tanski, J. M.; Waterman, R. A general synthesis of phosphaalkenes at zirconium with liberation of phosphaformamides. *Dalton Trans* **2013**, *42* (4), 1159-1167, 10.1039/C2DT32322B.

(25) Roering, A. J.; Leshinski, S. E.; Chan, S. M.; Shalumova, T.; MacMillan, S. N.; Tanski, J. M.; Waterman, R. Insertion Reactions and Catalytic Hydrophosphination by Triamidoamine-Supported Zirconium Complexes. *Organometallics* **2010**, *29* (11), 2557-2565.

(26) Vilanova, S. P.; del Rosal, I.; Tarlton, M. L.; Maron, L.; Walensky, J. R. Functionalization of Carbon Monoxide and tert-Butyl Nitrile by Intramolecular Proton Transfer in a Bis(Phosphido) Thorium Complex. *Angewandte Chemie International Edition* **2018**, *57* (51), 16748-16753, <https://doi.org/10.1002/anie.201810511>.

(27) Ghebreab, M. B.; Newsham, D. K.; Waterman, R. Differences in the stability of zirconium(IV) complexes related to catalytic phosphine dehydrocoupling reactions. *Dalton Trans* **2011**, *40* (30), 7683-7685, 10.1039/C1DT10105F.

(28) Liwosz, T. W.; Chemler, S. R. Copper-catalyzed oxidative amination and allylic amination of alkenes. *Chemistry* **2013**, *19* (38), 12771-12777.

(29) Alt, H.; Rausch, M. D. Photochemical reactions of dimethyl derivatives of titanocene, zirconocene, and hafnocene. *Journal of the American Chemical Society* **2002**, *96* (18), 5936-5937.

(30) Pinkas, J.; Wang, T.; Jacobson, R. A.; Verkade, J. G. Azaaluminatranes Exhibiting Unusual Coordination Geometries for Aluminum. *Inorganic Chemistry* **2002**, *33* (19), 4202-4210.

(31) Ketley, A. D.; McClanahan, J. L. The Rearrangement of 1-para-Substituted Phenyl-1-cyclopropylethylenes. *The Journal of Organic Chemistry* **2002**, *30* (3), 942-943.

